Journal of the Korean Crystal Growth and Crystal Technology
Vol. 25, No. 4 (2015) 160-165
http://dx.doi.org/10.6111/JKCGCT.2015.25.4.160

p-ISSN 1225-1429
e-ISSN 2234-5078

Processing, structure, and properties of lead-free piezoelectric NBT-BT

Sungwook Mhin, Jung-Il Lee* and Jeong Ho Ryu*,†

Heat Treatment R&D Group, Korea Institute of Industrial Technology, Cheonan 429-846, Korea
**Department of Materials Science and Engineering, Korea National University of Transportation, Chungju 380-702, Korea*

(Received July 30, 2015)
(Revised August 12, 2015)
(Accepted August 17, 2015)

Abstract Lead-free piezoelectric materials have been actively studied to substitute for conventional PZT based solid solution, $Pb(Zr_xTi_{1-x}O_3)$, which occurs unavoidable PbO during the sintering process. Among them, Bismuth Sodium Titanate, $Na_{0.5}Bi_{0.5}TiO_3$ (abbreviated as NBT) based solid solution is attracted for the one of excellent candidates which shows the strong ferroelectricity, Curie temperature (Tc), remnant polarization (Pr) and coercive field (Ec). Especially, the solid solution of rhombohedral phase NBT with tetragonal perovskite phase has a rhombohedral - tetragonal morphotropic phase boundary. Modified NBT with tetragonal perovskite at the region of MPB can be applied for high frequency ultrasonic application because of not only its low permittivity, high electrocoupling factor and high mechanical strength, but also effective piezoelectric activity by poling. In this study, solid state ceramic processing of NBT and modified NBT, $(Na_{0.5}Bi_{0.5})_{0.93}Ba_{0.7}TiO_3$ (abbreviated as NBT-7BT), at the region of MPB using 7 % $BaTiO_3$ as a tetragonal perovskite was introduced and the structure between NBT and NBT-7BT were analyzed using rietveld refinement. Also, the ferroelectric and piezoelectric properties of NBT-7BT such as permittivity, piezoelectric constant, polarization hysteresis and strain hysteresis loop were compared with those of pure NBT.

Key words NBT-7BT, Ferroelectric properties, Piezoelectric properties

1. Introduction

To date, the dominant piezoceramic has been lead zirconate titanate ($Pb(Zr_{1-x}Ti_x)O_3$ or PZT), because it shows excellent piezoelectric properties [1]. However, as its applications have expanded, environmental concern is also increasing due to the volatilization of PbO during processing, as well as recycling and waste disposal issues [2]. This has resulted in the exploration of Pb-free materials to substitute for PZT in current and developing piezoelectric applications [3-8].

Amongst the candidates to substitute for the conventional PZT, $(Na_xBi_{1-x})_yBa_{1-y}TiO_3$ (NBT-BT) is one of the most promising. [9] However, $(Na_xBi_{1-x})_yBa_{1-y}TiO_3$ (NBT) in the undoped form shows a high coercive field, which makes poling difficult. Also, its ferroelectric properties are not competitive with PZT. When NBT is modified using dopants such as $BaTiO_3$, and is near the MPB ($(Na_{0.5}Bi_{0.5})_{0.93}Ba_{0.7}TiO_3$), it has the potential for improved properties: higher mechanical strength, higher electro-mechanical coupling factor and effective piezoelectric activity by poling [10].

†Corresponding author
Tel: +82-43-841-5384
Fax: +82-43-841-5380
E-mail: jhryu@ut.ac.kr

In this study, $(Na_{0.5}Bi_{0.5})_{0.93}Ba_{0.7}TiO_3$ (NBT-7BT) was prepared via solid state processing. The properties of the NBT-7BT were compared with those of undoped $Na_{0.5}Bi_{0.5}TiO_3$ (NBT).

2. Experimental Procedure

2.1. Sample preparation

NBT was fabricated using the raw powders: sodium carbonate, titanium dioxide, bismuth oxide. The information about the raw powders is provided in Table 1.

The NBT-7BT was synthesized using following method; raw powders of sodium carbonate, titanium dioxide, bismuth oxide, and barium carbonate were used to synthesize NBT-7BT. Details of the starting powders are provided in Table 2.

Before weighing the raw powders, the sodium carbonate and barium carbonate were dried at 150°C for 1 h. The starting powders were weighed in stoichiometric amounts and placed in a 16 ounce Nalgene bottle containing 300 gm of 5 mm diameter, spherical zirconia milling media and 100 ml of ethanol and ball milled for 48 h. The powders were then dried for 24 h in an oven at 100°C. The dried powders were ground in a mortar

Table 1
Starting powders, companies, purities, molar fraction, molar weight, and weight used in synthesis of NBT

Composition	Company	Purity	Molar fraction	Molar weight (g/mol)	Weight used (g)
Na_2CO_3	Alfa aesar	99.5 %	0.25	105.99	1.2634
TiO_2	Fisher scientific	99.85 %	1	79.87	3.7785
Bi_2O_3	Alfa aesar	99.975 %	0.25	465.9	5.5108

Table 2
Starting powders, companies, purities, molar fraction, molar weight, and weight used in synthesis of NBT-7BT

Composition	Company	Purity	Molar fraction	Molar weight (g/mol)	Weight used (g)
Na_2CO_3	Alfa aesar	99.5 %	0.2325	105.99	1.1609
TiO_2	Fisher scientific	99.85 %	1	79.87	3.8994
Bi_2O_3	Alfa aesar	99.975 %	0.2325	465.9	5.0792
$BaCO_3$	Alfa aesar	99.8 %	0.07	197.35	0.6474

and pestle and were passed through 200 μm STM sieve.

The powders were calcined in a closed alumina crucible using a heating rate of 5°C/min up to 900°C, held for 3 h at 900°C and cooled at a rate of 4°C/min. The calcined powders were placed in a 16 ounce Nalgene bottle containing 300 gm of 5 mm spherical zirconia milling media, and 100 ml of ethanol and ball milled for 24 h. The powders were then dried for 24 h in an oven at 100°C and ground in a mortar and pestle with 1 gm of PVA binder.

0.4 g of the powder and binder mixture was loaded into a 10 mm diameter die and pressed into pellets using a uniaxial stress of 35 MPa. The pellets were then loaded into balloons, the balloons were evacuated of air, the ends tied, and the balloons were placed in the isostatic press under a 200 MPa stress for 2 min. Following this, the pellets were placed in a covered alumina crucible and sintered at 1150°C for 3 h after holding at 400°C for 1 h. The heating rate up to sintering temperature was 5°C/min and the cooling rate down to room temperature was 5°C/min. Both undoped NBT and NBT-7BT were made using this process.

2.2. Characterization

The density of the sintered pellets was measured using the Archimedes principle. The fluid used for the experiments was water and the measurements were performed at an ambient temperature of 25.1°C. Powder X-ray diffraction patterns of the pellets were recorded using a laboratory X-ray diffractometer equipped with a curved position sensitive detector (CPS 120, Inel), CuKα1 radiation, and multi-layer mirror optics for increased intensity. The surface of each pellet was investigated using SEM. Before the SEM observation, the samples were polished using diamond paste on the glass plate for improving the effect of thermal etching and then, thermal etching was performed, so that a reliable quantitative estimate of grain size could be achieved. Thermal etching was performed at the different conditions. The conditions were 1000°C for 10 min, 1000°C for 30 min, 1050°C for 10 min and 1050°C for 30 min and the optimal conditions for thermal etching were 1000°C for 10 min. With the other conditions, grain growth was observed after thermal etching. For electrical poling of the samples, the surfaces of pellets were cleaned with acetone and ethanol. Gold electrodes were deposited on the top and bottom surfaces using Gold sputter. The electrodes were of the same planar dimensions as the samples. Electrical poling was performed on pellets in an oil bath heated to 60°C. The samples were poled using the conditions listed in Table 3.

The direct, longitudinal piezoelectric coefficient (d_{33}) was measured using a wide-range Berlincourt d_{33} meter (model 90-2030, APC Ceramics) both immediately after poling and 10 days after poling. Also, the perpendicular piezoelectric coefficient (d_{31}) to the polarization direction was measured using a Berlincourt d_{31} meter immediately after poling. Polarization and strain hysteresis of a poled sample from undoped NBT and NBT-7BT were measured at a frequency of ~1 Hz under 8 kV/mm. Also, impedance and series resonance frequency of the pellets was measured using an Agilent 4294A Precision

Table 3
The conditions in undoped NBT and NBT-7BT pellets

	Thickness (mm)	Voltage (kV)	Field (kV/mm)	Time (min)
NBT	1.19	7.2	6.05	10
NBT-7BT	1.33	8	6.01	10

Impedance Analyzer. Dielectric permittivity of pellets was calculated using capacitance measured from pellets using an Agilent 4284A Precision LCR meter.

3. Results and Discussion

Relative densities of the undoped NBT and NBT-7BT were shown in Table 4. The relative density calculations were based on the theoretical density of undoped NBT and NBT-7BT, 5.99 g/cm^3 and 5.92 gm/cm^3, respectively. The equation used to calculate absolute density is:

$$p = \frac{w(a) * p(fl)}{0.99983G} + 0.0012$$

where w(a) - the weighed mass of pellet in air
p(fl) - density of fluid (H_2O at 25.1°C, p(fl) is 0.99707.)
G = w(a) – w(fl)

Table 4
Sample weight and density calculations of NBT and NBT-7BT

	Weight in air (g)	Weight in water (g)	Calculated absolute density (g/cm^3)	Relative density (%)
NBT	0.3676	0.3048	5.84098	97.51
NBT-7BT	0.392	0.3233	5.6914	96.05

The densities of undoped NBT and NBT-7BT were 97.51 % and 96.05 %, respectively.

Diffraction patterns of the powders were obtained from the surface of sintered pellets of undoped NBT and NBT-7BT. Selected diffraction patterns of sintered pellets are shown in Fig. 1(a). Both the upper and lower surfaces of each pellet were measured and the diffraction patterns obtained were very similar.

The diffraction patterns of NBT-7BT were analyzed using the Rietveld refinement program RIETICA. The space group R3m was used in the calculated patterns, and the difference of patterns below shows that this matches the experimental data closely (see Fig. 1(b)). Other space groups were attempted, each with a worse fit to the experimental pattern. The lattice parameters obtained from the refinement are a = 5.537675 Å and c = 6.7929 Å (in the hexagonal setting). This converts to a = 3.91779 Å and $\alpha = 89.9399^{\circ}$ in the rhombohedral

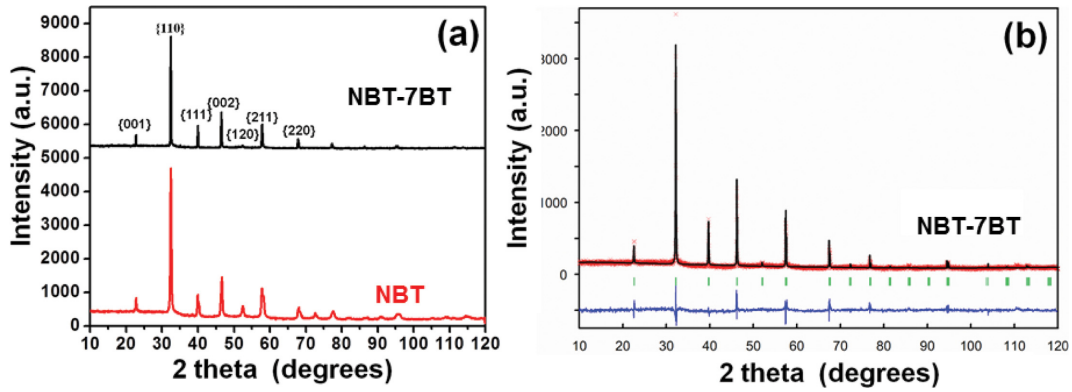

Fig. 1. (a) XRD patterns of sintered NBT and NBT-7BT pellets and (b) Rietveld refinement of NBT-7BT.

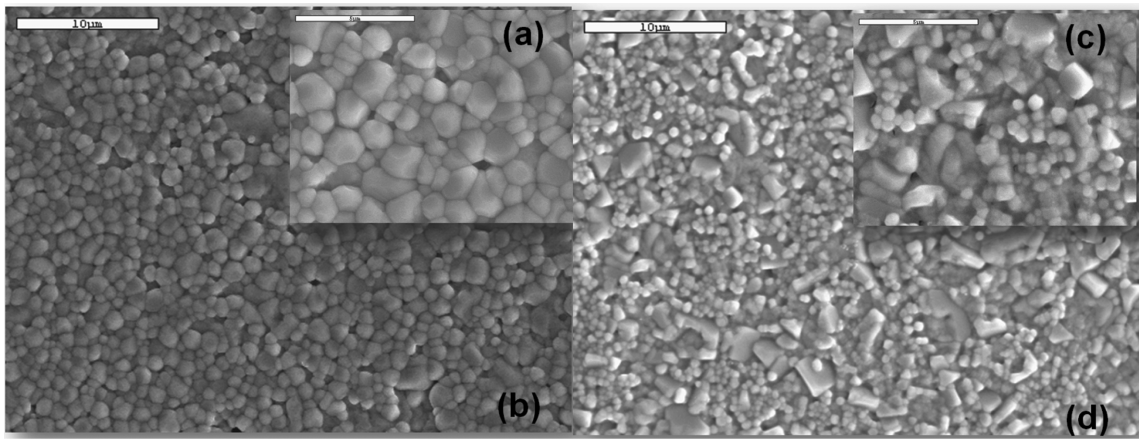

Fig. 2. Scanning electron micrographs of (a), (b) NBT and (c), (d) NBT-7BT.

setting. NBT-7BT powders show no second phases observed by XRD, indicating the samples are phase-pure. The sintered pellets have a homogeneous crystal structure throughout, which is shown by comparing the diffraction patterns of top and bottom surface of pellets.

Representative secondary electron micrographs of samples after thermal etching at the optimal conditions are shown in Fig. 2. The micrographs of undoped NBT (Fig. 2 (a), (b)) show homogeneous size distribution of grains which range from 500 nm to 3 μm, while less homogeneous size distribution of grains in the NBT-7BT (Fig. 2 (c), (d)) is shown.

The measured d_{31} and d_{33} values for NBT and NBT-7BT are shown in Table 5. The value of d_{33} in NBT-7BT pellet was almost twice higher than the undoped NBT. Also, d_{31} of the NBT-7BT was higher than the undoped NBT. However, decrease of the d_{33} and d_{31} was observed in the NBT-7BT, while no change of piezoelectric coefficient was observed in undoped NBT after 10 days.

The capacitance, dielectric permittivity and piezoelectric voltage constants of samples are shown in Fig. 3. The equation used to calculate dielectric permittivity is:

$$\varepsilon^{T}_{r,\,33} = \frac{t * C}{S * \varepsilon_0}$$

where t - thickness (m)

S - Area of covered electrodes (m^2)

C - Capacitance

ε_0 - dielectric permittivity in air (8.85*10-12 F/m)

Also, piezoelectric voltage constants (g_{31}, g_{33}) were calculated using the equation:

$$g_{33} = \frac{d_{33}}{\varepsilon_0 * \varepsilon^{T}_{r,\,33}}$$

$$g_{31} = \frac{d_{31}}{\varepsilon_0 * \varepsilon^{T}_{r,\,33}}$$

As shown in Table 6, the values of the capacitance and dielectric permittivity of the NBT-7BT were larger than those of undoped NBT.

The strain and the hysteresis loop from each sample

Table 5
The value of d_{33} and d_{31} in undoped NBT and NBT-7BT pellets

	d_{33} after poling (pC/N)	d_{33} after 10 days (pC/N)	d_{31} after poling (pC/N)	d_{31} after 10 days (pC/N)
NBT	72/–70	71/–69	–34	–31
NBT-7BT	143/–138	130/–128	–43	–39

Table 6
The conditions and value of dielectric permittivity and g_{33}/g_{31} of NBT and NBT-7BT pellets

	Thickness (m)	The area of sample electrode (m^2)	Capacitance (F)	Dielectric permittivity	g_{33} (Vm/N)	g_{31} (Vm/N)
NBT	0.001	0.00001592	170	384.266866	0.02143	0.01039
NBT-7BT	0.0013	0.00005338	248.27	683.2	0.02074	0.00612

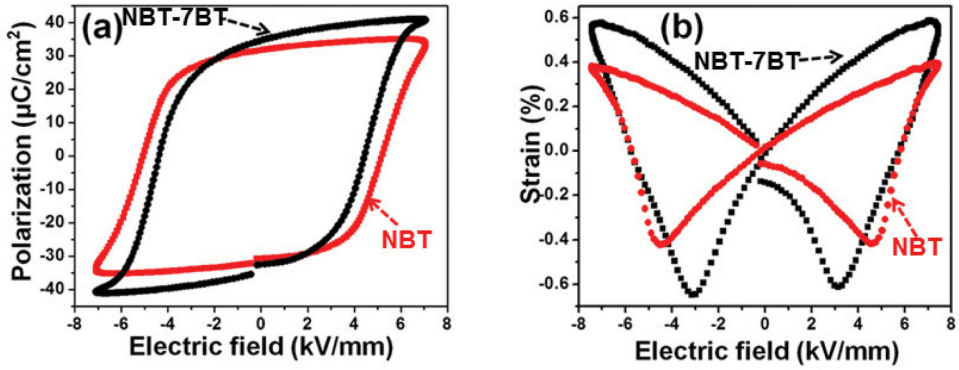

(c)

	E_c (kV/mm)	P_r (μC/cm²)	S_{max} (%)	S_r (%)
NBT	4.9203	19.1528	0.8	0.4223
NBT-7BT	3.8281	18.315	1.286	0.6447

Fig. 3. (a) Polarization, (b) strain loops for NBT and NBT-7BT and (c) piezoelectric properties of undoped NBT and NBT-7BT pellets.

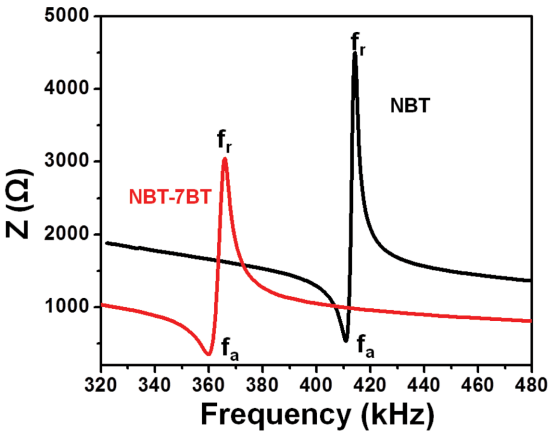

	f_r (kHz)	f_a (kHz)	f_r-f_a (kHz)	Planar coupling factor (k_p)
NBT	414.4202	411.0611	3.3591	0.1428
NBT-7BT	365.9416	359.4802	6.4614	0.2116

Fig. 4. Impedence value and planar coupling factor of NBT and NBT-7BT as a function of frequency.

were shown in Fig. 3. The coercive field from the hysteresis loop (Fig. 3(a)) shows the NBT-7BT has lower coercive field than undoped NBT. In the strain hysteresis measurements (Fig. 3(b)), the NBT-7BT shows larger strain than pure NBT under electrical field. Piezoelectric properties of both pellets are summarized in Fig. 3(c).

Fig. 4 shows the impedance from each sample as a function of frequency. Also, it shows details of resonance and anti-resonance frequencies of impedance of samples. The planar coupling (k_p) factors of the samples in the table below were calculated using the following approximation:

$$k_p = \sqrt{2.51\left(\frac{f_a - f_r}{f_a}\right) - \left(\frac{f_a - f_r}{f_a}\right)^2}$$

The results show that the planar coupling (k_p) of NBT-7BT is higher than that of undoped NBT. Also, the value of the planar coupling factor of each sample is comparable to reported values [1].

Table 7 shows the resonance frequency and frequency constant of both NBT and NBT-7BT. The frequency constant (N_p) of each samples was calculated using the following equation:

$$N_p = f_r \cdot D$$

Table 7
Frequency constant of undoped NBT and NBT-7BT pellets

	Diameter (m)	f_r (kHz)	N_p (m/s)
NBT	0.007909	411.0612	3251.283
NBT-7BT	0.00806	359.4802	2897.33

where D : diameter of ceramic element
f_r : resonant frequency

4. Summary

NBT and NBT-7BT pellets were prepared using solid solution processing. NBT-7BT shows lower coercive field, higher piezoelectric coefficient, higher dielectric permittivity and higher planar coupling factor than undoped NBT. This work confirms that the use of the materials with compositions close to morphotropic phase boundaries can be advantageous to the improvement of piezoelectric properties.

Acknowledgement

This research was supported by a grant from the School of Convergence Program of Ministry of Education.

References

[1] V.T. Tung, N.T. Tinh, T.V. Chuong, N.T.M. Huong, D.A. Tuan and L.V. Truyen, “Investigation the dimensional ratio effect on the resonant properties of piezoelectric ceramic disk”, J. Modern Phys. 4 (2013) 1627.
[2] D. Akai, R. Yoshita and M. Ishida, “(Na, Bi)TiO_3 based lead-free ferroelectric thin films on Si substrate for pyroelectric infrared sensors”, J. Phys.: Conference Series 433 (2013) 012017-1-6.
[3] M. Cernea, B.S. Vasile, C. Capiani, A. Ioncea and C. Galassi, “Dielectric and piezoelectric behaviors of NBT-$BT_{0.05}$ processed by sol–gel method”, J. Eur. Ceram. Soc. 32 (2012) 133.
[4] M. Chen, Q. Xu, B.H. Kim, B.K. Ahn and W. Chen, “Effect of CeO_2 addition on structure and electrical properties of $(Na_{0.5}Bi_{0.5})_{0.93}Ba_{0.07}TiO_3$ ceramics prepared by citric method”, Mater. Res. Bull. 43 (2008) 1420.
[5] H. Wang, R. Zuo, X. Ji and Z. Xu, “Effects of ball milling on microstructure and electrical properties of sol-gel derived $(Na_{0.5}Bi_{0.5})_{0.94}Ba_{0.06}TiO_3$ piezoelectric ceramics”, Mater. Des. 31 (2010) 4403.
[6] A. Ullah, C.W. Ahn, A. Hussain and I.W. Kim, “The effects of sintering temperatures on dielectric, ferroelectric and electric field-induced strain of lead-free $Bi_{0.5}(Na_{0.78}K_{0.22})_{0.5}TiO_3$ piezoelectric ceramics synthesized by the sol gel technique”, Curr. Appl. Phys. 10 (2010) 1367.
[7] H. Takahashi, Y. Numamoto, J. Tani, K. Matsuta, J. Qiu and S. Tsurekawa, “Lead-free barium titanate ceramics with large piezoelectric constant fabricated by microwave sintering”, Jpn. J. Appl. Phys. 45 (2006) L30-2.
[8] H.D. Li, C. Feng and W.L. Yao, “Some effects of differ-

ent additives on dielectric and piezoelectric properties of $(Na_{1/2}Bi_{1/2})TiO_3$-$BaTiO_3$ morphotropic-phase-boundary composition", Mater. Lett. 58 (2004) 1194.
[9] J. Rodel, W. Jo, K.T.P. Seifert, E. Anton and T. Granzow, "Perspective on the development of lead-free piezoceramics", J. Amer. Ceram. Soc. 92 (2009) 1153.
[10] T. Tanaka, K. Maruyama and K. Sakata, "$(Bi_{0.5}Na_{0.5})TiO_3$-$BaTiO_3$ system for lead-free piezoelectric ceramics", Jpn. J. Appl. Phys. 30 (1991) 2236.